Krypton-81 in Groundwater of the Culebra Dolomite Near the Waste Isolation Pilot Plant, New Mexico

Neil C. Sturchio[1*], Kristopher L. Kuhlman[2], Reika Yokochi[1,3], Peter C. Probst[1], Wei Jiang[4], Zheng-Tian Lu[4,5], Peter Mueller[4], Guo-Min Yang[4,6]

[1]Department of Earth and Environmental Sciences, University of Illinois at Chicago, Chicago, IL 60607, USA

[2]Repository Performance Department, Sandia National Laboratories, Carlsbad, NM 88220 USA

[3]Department of Geophysical Sciences, The University of Chicago, Chicago, IL 60637, USA

[4]Physics Division, Argonne National Laboratory, Argonne, IL 60439, USA

[5]Department of Physics and Enrico Fermi Institute, The University of Chicago, Chicago, IL 60637, USA

[6]Hefei National Laboratory for Physical Sciences at Microscale, University of Science and Technology of China, Hefei, Anhui 230026, China

*Corresponding author: Sturchio@uic.edu; 312-355-1182; 845 West Taylor Street, MC-186, Chicago, IL 60607-7059

ABSTRACT

The Waste Isolation Pilot Plant (WIPP) in New Mexico is the first geologic repository for disposal of transuranic nuclear waste from defense-related programs of the US Department of Energy. It is constructed within halite beds of the Permian-age Salado Formation. The Culebra Dolomite, confined within Rustler Formation evaporites overlying the Salado Formation, is a potential pathway for radionuclide transport from the repository to the accessible environment in the human-disturbed repository scenario. Although extensive subsurface characterization and numerical flow modeling of groundwater has been done in the vicinity of the WIPP, few studies have used natural isotopic tracers to validate the flow models and to better understand solute transport at this site. The advent of Atom-Trap Trace Analysis (ATTA) has enabled routine measurement of cosmogenic ^{81}Kr (half-life 229,000 yr), a near-ideal tracer for long-term groundwater transport. We measured ^{81}Kr in saline groundwater sampled from two Culebra Dolomite monitoring wells near the WIPP site, and compared ^{81}Kr model ages with reverse particle-tracking results of well-calibrated flow models. The ^{81}Kr model ages are ~130,000 and ~330,000 yr for high-transmissivity and low-transmissivity portions of the formation, respectively. Compared with flow model results which indicate a relatively young mean hydraulic age (~32,000 yr), the ^{81}Kr model ages imply substantial physical attenuation of conservative solutes in the Culebra Dolomite and provide limits on the effective diffusivity of contaminants into the confining aquitards.

1. INTRODUCTION

The Waste Isolation Pilot Plant (WIPP) in southeastern New Mexico (Fig. 1) began accepting transuranic waste from the U. S. Department of Energy's defense-related nuclear programs in 1999, following 25 years of subsurface characterization studies (Mora, 1999). A key factor in the WIPP compliance certification decision by the U. S. Environmental Protection Agency (EPA) is the probability of radionuclide release to the accessible environment within 10,000 years (Helton et al., 1999; Swift and Corbet, 2000). Performance assessment of the WIPP repository for the compliance certification application involved numerical simulations and conceptual models based on extensive subsurface characterization and test data (Lambert, 1992; Beauheim and Ruskauff, 1998; Meigs and Beauheim, 2001; Haggerty et al., 2001; McKenna et al., 2001; Kuhlman and Barnhart, 2011; U.S. DOE, 2014). These models and simulations considered past and future climate conditions and the long-term geochemical and hydrological evolution of the repository site.

The WIPP repository is located about 655 m below the surface in the Permian-age (~250 Ma) Salado Formation, which is a ~500-m thick deposit comprised mostly of bedded halite with thin interbeds of clay, anhydrite, and other salts (Fig. 2). The Salado Formation is overlain by the Permian-age Rustler Formation, which includes the regionally continuous and confined Culebra Dolomite (Fig. 2) (Swift and Corbet, 2000). The Culebra Dolomite, confined within Rustler Formation evaporites, is the most likely potential pathway for radionuclide transport from the repository to the accessible environment in the human-disturbed repository scenario, because it is the nearest conductive formation overlying the repository. The saline water in the Culebra Dolomite at the WIPP site is depleted in ^{2}H and ^{18}O relative to modern precipitation,

indicating meteoric recharge most likely occurred during humid climate periods of the Late Pleistocene (Lambert, 1992), in or near Nash Draw or Clayton Basin northwest of the WIPP site.

(figure 1 near here)

Past attempts to determine the timing of meteoric recharge of Culebra groundwater in the vicinity of the WIPP site using atmospheric tracers have been largely unsuccessful. Carbon-14 abundances in dissolved inorganic carbon from the Culebra groundwater were reported by Lambert (1987). Considering the evidence for ^{14}C contamination by introduction of modern carbon during well drilling and completion, the data were interpreted by Lambert (1987) to indicate a minimum, unadjusted ^{14}C model age about 12,000 to 16,000 years before present for the least-contaminated samples. This minimum age estimate is consistent with stable isotope ratios of water and other evidence for pre-Holocene recharge. The isotopic abundance of ^{36}Cl (half-life = 301,000 yr) in the Culebra water was below detection (i.e., $^{36}Cl/Cl < 1x10^{-15}$) (Lambert, 1987).

(Figure 2 near here)

Radiokrypton isotopes ^{81}Kr (half-life = 229,000 yr) and ^{85}Kr (10.8 yr) are near-ideal groundwater tracers because of their inert chemical behavior and well-known source terms (Collon et al., 2004), yet there are few published groundwater studies involving radiokrypton isotopes because of the difficulties associated with measuring such low-abundance isotopes (especially ^{81}Kr) (Lehmann et al., 2003; Sturchio et al., 2004). Krypton-81 is the best available groundwater tracer in the range of approximately 50,000 yr to 1,000,000 yr. Its atmospheric

abundance ($^{81}Kr/Kr \sim 10^{-12}$) is expected to be constant over millions of years and it has negligible subsurface production in low-U environments (Collon et al., 2004). Thus, ^{81}Kr is a particularly valuable tracer for old saline groundwater such as that present in the Culebra Dolomite, where ^{36}Cl is not a viable tracer of groundwater age because the meteoric component of ^{36}Cl is camouflaged by chloride introduced from halite dissolution and in situ production of ^{36}Cl (Phillips, 2000). Krypton-85 is somewhat more abundant than ^{81}Kr because of anthropogenic production in the nuclear fuel cycle ($^{85}Kr/Kr \sim 10^{-11}$), and its 10.8 yr half-life makes it an ideal tracer for young (<60 yr) groundwater and/or identification of air contamination during sampling of old groundwater.

Recent advances in the atom-trap trace analysis (ATTA) method (Chen et al., 1999), in particular the development of the 3rd-generation instrument ATTA-3 (Jiang et al., 2012), have enabled routine measurements of ^{81}Kr and ^{85}Kr. We used ATTA to obtain radiokrypton analyses for saline groundwater sampled from the Culebra Dolomite in two new monitoring wells near the WIPP site. These measurements provide important new constraints on long-term groundwater flow rates and solute transport in the vicinity of the WIPP repository. In addition, they provide an opportunity to evaluate the role of radiokrypton measurements in the long-term ($>10^4$ years) assessment of far-field repository performance.

2. SAMPLES AND METHODS

Two monitoring wells screened in the Culebra Dolomite were sampled for radiokrypton analysis during summer 2007. These wells, SNL-8 and SNL-14 (Fig. 1), were drilled and completed in May–June, 2005 (Powers, 2009; Powers and Richardson, 2008). Well SNL-8 intersects a relatively low-transmissivity (T) zone of the Culebra Dolomite ($T = 10^{-6.6}$ m^2/s)

whereas well SNL-14 intersects a relatively high-transmissivity zone ($T = 10^{-4.3}$ m^2/s) (Hart et al., 2008) Large-volume samples were collected by pumping several thousand liters of groundwater through a portable membrane-contactor apparatus that extracted the dissolved gas from the water and transferred it to a gas cylinder (Probst et al., 2007). The apparatus was leak-tested under negative pressure prior to sampling, and positive water pressure was maintained continuously during sampling to prevent contamination with air. Water quality samples were obtained by Sandia personnel and analyzed by EPA methods (or equivalent) at Hall Environmental Analysis Laboratory in Albuquerque, NM. In addition, water samples collected at the same time were provided to the U.S. Geological Survey in Reston (VA) were analyzed for tritium, ^{14}C, CFCs, SF_6, and other dissolved gases (Plummer and Busenberg, 2008).

Gas cylinders were returned to the Environmental Isotope Geochemistry Laboratory at the University of Illinois at Chicago (UIC), where bulk gas compositions were measured by quadrupole mass spectrometry using a SRS-200 residual gas analyzer using atmospheric air as a reference gas. Krypton was extracted from the bulk gas at UIC by cryogenic distillation and gas chromatography (Yokochi et al., 2008), and the isotope ratios ^{81}Kr/^{83}Kr and ^{85}Kr/^{83}Kr were determined using the ATTA-3 instrument in the Laboratory for Radiokrypton Dating, Argonne National Laboratory (Jiang et al., 2012). Based on the Atom Trap Trace Analysis method (Chen et al., 1999), ATTA-3 is a selective and efficient atom counter capable of measuring both ^{81}Kr/Kr and ^{85}Kr/Kr ratios of environmental samples in the range of 10^{-14} – 10^{-10}. In the apparatus, atoms of a targeted isotope (^{81}Kr, ^{85}Kr, and the control stable isotope ^{83}Kr) are captured by resonant laser light into an atom trap, and counted by observing the fluorescence of the trapped atoms. For ^{81}Kr dating in the age range of 150 kyr – 1,500 kyr, the required sample size is 5 – 10 micro-L STP of krypton gas, which can be extracted from approximately 100 – 200

kg of water or 40 – 80 kg of ice. For ^{85}Kr dating of young groundwater, the required sample size is generally a factor of 10 less. Both the reliability and reproducibility of the method were examined with an inter-comparison study among different methods and instruments. The ^{85}Kr/Kr ratios of 12 samples, in the range of 10^{-13} to 10^{-10}, were measured independently in three laboratories: a low-level counting laboratory in Bern, Switzerland, and two ATTA laboratories, one in Argonne and the other in Hefei, China. The results are in agreement at the precision level of 7% (Jiang et al., 2012; Yang et al., 2013). For quality control in the analysis of environmental samples, the instrument is calibrated with a standard modern atmospheric Kr sample both before and after the analysis of a group of two or three environmental samples. The detection limit of ATTA-3, defined as the lowest isotope ratio detectable by ATTA-3, is approximately 2 dpm/cc for ^{85}Kr/Kr. This detection limit, caused by the instrument memory effect, was determined with repeated measurements of a ^{85}Kr-dead sample. Here we use the conventional units of dpm/cc, which stands for the number of ^{85}Kr disintegrations per minute per mL-STP of Kr gas. For conversion, 100 dpm/cc corresponds to the ^{85}Kr/Kr ratio of 3.03×10^{-11}. We report ^{81}Kr isotopic abundance in groundwater normalized to that of modern atmospheric air which has ^{81}Kr/Kr = $5.2(\pm 0.4) \times 10^{-13}$ (Collon et al., 2004). We define the value $^{81}R_{gw} = (^{81}\mathrm{Kr/Kr})_{sample}/(^{81}\mathrm{Kr/Kr})_{atm}$.

3. RESULTS

Compositions of gas and water samples are given with information about wells and sampling parameters in Table 1. Extracted gases are about 97–98 vol. % N_2 with minor amounts of Ar, CO_2, CH_4 and O_2. Water samples have high salinity (SNL-14: 87,000 and SNL-8: 140,000 mg L^{-1}) derived mainly from halite dissolution (Lambert, 1992; Siegel and Anderholm, 1994). Isotopic abundances of ^{81}Kr in the well water samples are low relative to modern

atmospheric air, indicating that subsurface residence times are substantial relative to the 229,000-yr half-life of ^{81}Kr. The presence of measurable ^{85}Kr in sample from SNL-8 indicates apparent admixture of some modern atmospheric Kr introduced during well completion, and requires correction to obtain the characteristic ^{81}Kr isotopic abundance of the groundwater in the Culebra Dolomite, as discussed in the following section. Tritium activities in water samples from both wells are low (0.1 ± 0.1 TU), indicating little or no mixing with post-bomb water. Carbon-14 activities in dissolved inorganic carbon were 13.1 and 7.1 in SNL-8 and SNL-14, respectively; these values are inconsistent with the long residence times implied by $^{81}Kr/Kr$ ratios, and most likely indicate contamination by carbon additives introduced during drilling and well completion as discussed by Lambert (1987) and Plummer and Busenberg (2008).

4. DISCUSSION

The use of isotopic tracers in conjunction with accurately parameterized flow and transport models is generally a valuable approach for understanding large-scale flow systems within aquifers (Bethke and Johnson, 2008). Extensive effort has been invested in characterization, testing, and modeling of groundwater flow and tracer transport within the Culebra Dolomite, resulting in an ensemble of calibrated flow models that have been used in performance assessment and certification of the WIPP repository (U.S. DOE, 2014). The ^{81}Kr data can be evaluated in the context of these flow models to provide new insights regarding solute transport in the Culebra Dolomite. Before comparing the ^{81}Kr data with the flow models, however, we first evaluate the ^{81}Kr data.

(Table 1 near here)

4.1 Evaluation of ^{81}Kr data

The low concentrations of O_2 in the extracted gas samples from SNL-8 and SNL-14 indicate negligible (<1%) contamination of samples by air during and after sampling. Dissolved O_2 concentrations in water samples collected in parallel with this study were ~0.1 mg/L (Plummer and Busenberg, 2008). The post-sampling integrity of our gas samples was ensured by positive pressure within the gas cylinders (5.2 bar for SNL-8, 7.2 bar for SNL-14). However, the use of imported water with carbon-rich drilling additives such as PolyBore™ QuikFoam™, and soda ash, and air jetting during well drilling and completion (Powers, 2009; Powers and Richardson, 2008), apparently introduced some modern atmospheric tracers (e.g., CFCs, SF_6, ^{14}C) into the boreholes (Plummer and Busenberg, 2008). The low tritium activities of the well waters collected at the time of sampling for this study (0.1 $\pm$0.1 TU) indicate a minimal fraction of young (post-bomb) water in the samples, but the presence of the modern atmospheric tracers indicates that we must be concerned with possible introduction of modern atmospheric Kr.

Fortunately, the extent of possible modern atmospheric Kr contamination can be readily assessed from the measured activities of ^{85}Kr in our samples. The relatively short ^{85}Kr half-life (~10.8 yr) and its negligible subsurface production (Collon et al., 2004) indicate that ^{85}Kr should be undetectable in the aquifer water because the groundwater residence time is much greater than the ^{85}Kr half-life (e.g., the mean hydraulic age of Culebra water in SNL-14 in 32,100 yr, according to the flow model results). We detected ^{85}Kr activity in the sample from SNL-8, but none was detected in the sample from SNL-14 (Table 1). We therefore assume that the ^{85}Kr in SNL-8 was most likely introduced during drilling and well completion, which would constrain the ^{85}Kr isotopic abundance of the introduced Kr to have been equal to that of atmospheric Kr at the time of well completion. The absence of ^{85}Kr in SNL-14 may reflect the fact that a large-

scale pumping test (with 3.6×10^6 L water extracted by continuous pumping over 22 days) was performed in SNL-14 during late 2005 (Kuhlman and Barnhart, 2011), and this may have effectively flushed out any modern atmospheric Kr that had been introduced into the Culebra during drilling and well completion. No such large-scale pumping test was done in SNL-8, because of the low transmissivity of the Culebra at that location.

A decay correction gives the ^{85}Kr isotopic abundance for SNL-8 at the time of sampling (Table 1). The corrected ^{85}Kr isotopic abundance for SNL-8 can be used to correct the ^{81}Kr isotopic abundance as follows. First, we assume that ^{81}Kr in the undisturbed Culebra was incorporated by saturation with air at the time of recharge (t = 0). We also assume that the isotopic abundance of ^{81}Kr in air has been constant over the time scale of Culebra recharge and transport, and that atmospheric Kr is well mixed, thus the *initial* ^{81}Kr isotopic abundance in the Culebra groundwater was equal to that of modern atmospheric Kr (i.e., ^{81}Kr/Kr ≈ 5 x 10^{-13}). The Kr extracted from SNL-8 had ^{85}Kr activity = 10.3 ± 0.8 dpm/cc when analyzed on 21 November 2011. This value converted to ^{85}Kr isotopic abundance (^{85}Kr/Kr) at the time of well completion is 4.71 (± 0.37) × 10^{-12}. The isotopic abundance of ^{85}Kr in northern hemisphere air at the time of well completion (summer 2005) was 2.32×10^{-11} (Momoshima et al., 2010), which is only slightly lower than that during sampling in summer 2007 which was 2.48×10^{-11} (Dubasov and Okunev, 2010). As noted above, the most likely time of mixing of atmospheric Kr into SNL-8 was during well completion, and the pre-drilling formation water likely had negligible ^{85}Kr activity. Therefore, we can estimate both the fraction F_{atm} of atmospheric Kr mixed into the groundwater at SNL-8 during well completion and the fraction F_{gw} of Kr present in the groundwater prior to drilling:

$$F_{atm} = 4.71 \pm 0.37 \times 10^{-12} / 2.32 \times 10^{-11} = 0.203 \pm 0.016, \text{ and} \quad (1)$$

$$F_{gw} = 1 - F_{atm} = 0.797 \pm 0.016 \quad (2)$$

Because F_{atm} has the ^{81}Kr isotopic abundance of modern atmospheric air, the corrected ^{81}Kr isotopic abundance of F_{gw} (i.e., $^{81}R_{gw}$) in sample SNL-8 can be obtained from the measured value (0.50 ± 0.04) as follows:

$$0.50 \pm 0.04 = F_{atm} R_{atm} + F_{gw}\, {}^{81}R_{gw} = 0.203 \pm 0.016 + (0.797 \pm 0.016 \times {}^{81}R_{gw}) \quad (3)$$

and therefore $^{81}R_{gw} = 0.37 \pm 0.05$. (4)

4.2 Estimation of ^{81}Kr Model Ages

Groundwater "age" can be defined in concept as the mean subsurface residence time elapsed since isolation of a given volume of water from the atmosphere, keeping in mind that each H_2O molecule in that volume may have a different residence time (Bethke and Johnson, 2008). In practice, however, determination of age from tracer measurements generally becomes more difficult with increasing time because of the physical effects of mixing, dispersion, and diffusion, and in the case of a reactive tracer, the effects of chemical reactions within the aquifer. Although there are a number of fairly well-established tracers for young groundwater (i.e. < 60 years), including tritium, ^{3}H/^{3}He, chlorofluorocarbons (CFCs), SF_6, and ^{85}Kr (Newman *et al.*, 2010), there are fewer tracers suitable for older groundwater and all are to some extent problematic. Radiocarbon (^{14}C) is useful in the age range of ~1,000 to ~50,000 years, but calculated residence times can be highly model-dependent because of complications imparted by geochemical reactions involving carbonate minerals and production of biogenic CO_2 within the aquifer (e.g., Plummer and Sprinkle, 2001). For groundwater ages between ~50,000 and ~1,000,000 years, there are three available tracers – ^{4}He, ^{36}Cl, and ^{81}Kr (Suckow et al., 2013). As noted above, ^{81}Kr is the best available tracer for such old groundwater, because it is

nonreactive, and it has a well-known atmospheric source term and negligible subsurface production in low-U rocks such as the evaporites and carbonates of the Rustler Formation.

The simplest model for relating ^{81}Kr abundance to groundwater age assumes a closed system in which the $^{81}R_{gw}$ value of the sample represents a mixture of different groundwater ages. Thus the ^{81}Kr model age, which represents the apparent time elapsed between recharge and sampling (t), is given by:

$$t = -1/\lambda \ln (^{81}R_{gw}/[^{81}Kr/Kr_{atm}]) \quad (5)$$

where λ is the ^{81}Kr decay constant (3.03×10^{-6} yr^{-1}) and ^{81}Kr isotopic abundance in groundwater is expressed in terms of its atmosphere-normalized ratio, $^{81}R_{gw} = [^{81}Kr/Kr]_{sample}/[^{81}Kr/Kr]_{atm}$. The ^{81}Kr isotopic abundances of the sample and the atmosphere are both measured by ATTA. The $^{81}R_{gw}$ value for SNL-8 (corrected) is 0.37 ± 0.05, which yields a ^{81}Kr model age of 328 ($^{+48}/_{-41}$) × 10^3 yr, whereas the $^{81}R_{gw}$ value for SNL-14, 0.67 ± 0.05, yields a ^{81}Kr model age of 132 ($^{+26}/_{-23}$) × 10^3 yr. The ^{81}Kr model ages are qualitatively consistent with the relative transmissivities of the Culebra Dolomite in these two wells; the sample from the low-transmissivity well (SNL-8) has a higher ^{81}Kr model age than that of the sample from the high-transmissivity well (SNL-14).

4.3 Comparison of ^{81}Kr Model Ages with Flow Model Results

The flow model used for WIPP performance assessment is a Monte Carlo suite of 100 calibrated steady-state flow models (U.S. DOE, 2014). The initial model parameter guesses before calibration were stochastically-generated based on significant hydrologic and geologic data. Realizations were calibrated against transient and steady-state hydraulic head data. . The flow-field map shown in Fig. 3 is an average output across the realizations (U.S. DOE, 2014). A subset of this existing suite of calibrated models was used in the present study to produce 55

realizations with backtracked particles originating from the upstream model boundary in the direction of the presumed recharge area (R in Fig. 3) to well SNL-14. SNL-14 lies in a relatively high-transmissivity north-south zone south (downgradient) of the WIPP site (Fig. 3). Single-well pumping tests indicate Culebra transmissivity at SNL-14 ($10^{-4.3}$ m^2/s) is more than two orders of magnitude higher than at SNL-8 ($10^{-6.6}$ m^2/s) which is located in a low-transmissivity zone northeast (upgradient and lateral) of the WIPP site (Hart et al., 2008). As illustrated by the mean flow field in Fig. 3, SNL-8 is in a stagnant portion of the Culebra, which is bounded on the east by an irregular no-flow boundary inferred from the presence of halite in the Rustler Formation stratigraphically above and below the Culebra, which are equivalent to halite-free mudstones elsewhere to the west (Powers and Holt, 2000).

(Figure 3 hear here)

The Culebra does not outcrop or subcrop in the flow model area, or at the flow model boundaries. Particle tracking results therefore correspond to minimum possible groundwater ages. Meteoric recharge is believed to have occurred mainly either at the north end of Nash Draw or in Clayton Basin several km further to the north and west (Fig. 1). The predicted travel times from the upstream edge of the model domain at the northeastern end of Nash Draw ("R" in Fig. 3) to SNL-14 range from 9,500 to 141,000 yr, with a mean travel time of 32,100 yr and a mode at 20,900 yr, reflecting skewness to longer travel times (Fig. 4). The ^{81}Kr model age of 132 ($^{+26}/_{-23}$) $\times$ 10^3 yr for well SNL-14 is 4.1 times higher than the mean predicted flow model travel time from the upstream flow model boundary. The flow model age range defines a lower limit, given that the likely Culebra recharge area is beyond the upstream model boundary.

However, transmissivity is relatively high near the recharge area (Fig. 3), so the mean flow model travel times to SNL-14 would not increase greatly by extending the flow model boundary several km further north. For example, given a Darcy flow velocity of 10^{-6} or 10^{-7} m s^{-1}, extending the particle track 3.15 km further would add only 100 or 1,000 yr, respectively, to the flow model travel times for SNL-14.

For SNL-8, flow model-predicted directions and travel times were not used for comparison, because the low-flow area east and north of SNL-8 is not accurately described by purely advective flow on account of the relatively low Peclet numbers in this stagnant zone. The SNL-8 ^{81}Kr model age is consistent with a combination of advective and diffusive flow, which may transport water into the stagnant region at SNL-8 from the active north-south flow zone around the white asterisk in Fig. 3. This location is on average about 10,000 years upgradient from SNL-14. The time scale of this transport is dictated by the Darcy flow velocity in this portion of the Culebra, which is on the order of 10^{-8} m s^{-1}, and the diffusion coefficient of Kr in water (~2×10^{-9} m^2 s^{-1}, or 0.063 m^2 yr^{-1}, at 25°C) (Wise and Houghton, 1968; Jähne et al., 1987), which when adjusted for Culebra matrix tortuosity and porosity (Holt, 1997) gives an effective diffusivity of ~3×10^{-11} m^2 s^{-1}. The distance between SNL-8 and the asterisk in Fig. 3 is about 500 m, over which transport by advection at 10^{-8} m s^{-1} (i.e., 0.3 m yr^{-1}) could occur in about 1,700 yr, whereas diffusive transport at 3×10^{-11} m^2 s^{-1} would proceed only about 2.5 m in the same amount of time. Therefore, this pathway and a diffusion-dominated transport mechanism for both Kr and water are broadly consistent with the SNL-8 ^{81}Kr-based model age which is ~200,000 years older than that of SNL-14.

(Figure 4 near here)

4.4 Constraining Effective Diffusivity With ^{81}Kr

Detailed studies of porosity types in the Culebra Dolomite indicate that hydraulic conductivity is controlled mainly by the spatially heterogeneous distribution of interconnected small-scale fractures, vugs, and intercrystalline porosity (Holt, 1997; Meigs and Beauheim, 2001). Most of the advective flow occurs within the lower 4.4 m of the formation (Holt, 1997). Field-scale nonreactive tracer tests in the Culebra Dolomite (Meigs and Beauheim, 2001) indicate that a single-rate, double-porosity model (i.e., a model having a single diffusion rate through matrix porosity and advective transport through a network of interconnected fractures) is an adequate approximation at length scales beyond several km (Holt, 1997; McKenna et al., 2001). The geometry of the Culebra Dolomite, i.e. an extensive, relatively thin conductive layer sandwiched between relatively thick aquitards, is thus well suited for the application of steady-state analytical solutions developed initially for radionuclide transport along single fractures through a porous matrix (Grisak and Pickens, 1980; Neretnieks, 1980; Tang et al., 1981), and subsequently modified to estimate the effects of matrix diffusion on radiocarbon dating (Neretnieks, 1981; Sudicky and Frind, 1981; Maloszewski and Zuber, 1991; Sanford, 1997; Cook et al., 2005; Plummer and Glynn, 2013). Sudicky and Frind (1981) pointed out that the diffusive effect on tracer model ages would be larger for isotopes having longer half-lives than ^{14}C. The solution of Sanford (1997), as formulated by Plummer and Glynn (2013), can be conveniently used as follows to estimate the effect of matrix diffusion on ^{81}Kr model age in the Culebra Dolomite.

The effect on ^{14}C model age in a thin planar flow zone surrounded by thick, planar, ^{14}C-free stagnant zones with parallel boundaries can be expressed as:

$$t_c/t_u = k/(k + k_{diff}) \quad (6)$$

where t_c is the ^{14}C model age corrected for diffusion, t_u is the uncorrected ^{14}C model age, k is the radioactive decay constant of ^{14}C, and k_{diff} is defined as the diffusive loss constant,

$$k_{diff} = 2\,[(k\,D_{eff})^{0.5} / \varphi\, w_{flow}]\, \tanh\,[(w_{stag}/2)(k/D_{eff})^{0.5}] \quad (7)$$

where D_{eff} in $m^2\ yr^{-1}$ is the effective diffusion coefficient in the stagnant zone (which can be simply related to the aqueous diffusion coefficient D_{aq} by porosity, tortuosity, and adsorption factors), φ is the porosity of the flow zone, w_{flow} is the width in meters of the flow zone, and w_{stag} is the width in meters of the stagnant zone.

By setting k equal to the ^{81}Kr decay constant ($3.03 \times 10^{-6}\ yr^{-1}$), equations (6) and (7) predict the effect of diffusive exchange with stagnant zones on the ^{81}Kr model age of water in the Culebra Dolomite. Assuming fixed values of 0.15 and 4.4 m for φ and w_{flow}, respectively (Holt, 1997; Meigs and Beauheim, 2001), 0.063 $m^2\ yr^{-1}$ for D_{aq}, and arbitrarily varying D_{eff} and w_{stag} over reasonable ranges, we obtain the set of solutions shown in Figure 5. The asymptotic behavior seen as a function of w_{stag} in Fig. 5 is a consequence of the radioactive decay length of ^{81}Kr, which is the distance traveled by ^{81}Kr during its mean lifetime ($1/k$) and can be approximated in the stagnant zone as $(D_{eff}/k)^{0.5}$. Thus, for a steady-state model system as defined above, the value of t_u/t_c gives a lower limit on w_{stag}, and where φ and w_{stag} are known independently, t_u/t_c gives D_{eff}.

(Figure 5 near here)

By setting t_c equal to the mean value of the flow model travel times (32,100 yr) and t_u equal to the ^{81}Kr model age for SNL-14 (132,000 yr), we obtain t_u/t_c = 4.1 and D_{eff}/D_{aq} = 8.0 x 10^{-5} (Fig. 5). This yields a value for D_{eff} of 4.7 x 10^{-6} m^2 yr^{-1}, and a corresponding radioactive decay length of 1.6 m. For the mode value of the flow model travel times (20,900 yr), we obtain t_u/t_c = 6.3 and D_{eff}/D_{aq} = 2.3 x 10^{-4} (Fig. 5), which yields a value for D_{eff} of 1.4 x 10^{-5} m^2 yr^{-1}, and a corresponding radioactive decay length of 4.7 m. These radioactive decay lengths are much shorter than the known width of the stagnant zone around the Culebra; the nearest conductive stratigraphic unit is the Magenta Dolomite, which has hydraulic conductivity one to two orders of magnitude less than that of the Culebra Dolomite (Beauheim and Ruskauff, 1998) and is 30 m higher in the section. If the D_{eff} values were higher, the uncorrected ^{81}Kr ages would also be higher because of enhanced matrix diffusion; conversely, lower D_{eff} values yield lower uncorrected ^{81}Kr ages because of less efficient Kr exchange between the Culebra and its bounding aquitards. The low apparent values of D_{eff} are thus well-constrained by the hydrostratigraphy and, therefore, they imply low interconnected porosity in the stagnant zone and/or that Kr diffusivity is impeded by Kr adsorption on surfaces or perhaps by salt-induced solubility effects (e.g., Suckow and Sonntag, 1993). A salinity gradient decreasing toward the Culebra flow zone can be maintained by gradual dissolution of halite in the surrounding formations (Lambert, 1992; Siegel and Anderholm, 1994).

5. CONCLUSIONS

The transport of ^{81}Kr in Culebra Dolomite groundwater near the WIPP site has been examined by comparing ^{81}Kr model ages with hydraulic ages predicted by a well-calibrated flow model. The ^{81}Kr model age increases with decreasing Culebra transmissivity, and is substantially higher than mean hydraulic age in well SNL-14 where a direct comparison can be

made with flow model predictions. The disagreement between ^{81}Kr model age and flow model-predicted hydraulic age provides a constraint on the effective diffusivity of Kr in stagnant pore fluids of aquitard formations adjacent to the flow zone of the Culebra Dolomite. Calculated values of effective diffusivity of Kr in the stagnant zone, based on median and mean flow model-predicted travel times, are constrained to be on the order of 1.4×10^{-5} to 4.7×10^{-6} m^2 yr^{-1}. These low values imply that there is low interconnected porosity in the formations surrounding the Culebra flow zone and/or that Kr diffusivity is slowed by adsorption or salinity gradient effects..

The results described here show that application of ^{81}Kr measurements to groundwater age determinations in saline aquifers is possible but is complicated by the effects of diffusive exchange with surrounding aquitard formations. With sufficient information on the hydrogeology of the aquifer and surrounding aquitard formations, apparent ^{81}Kr model ages can be corrected to yield useful constraints on groundwater age. Conversely, with sufficiently accurate flow models, ^{81}Kr data can provide useful constraints on the effective diffusivity of surrounding aquitard formations. In either case, ^{81}Kr measurements appear to provide a valuable complement to other approaches used in the assessment of repository performance and far-field radionuclide transport of salt-hosted repositories as well as those in other geological settings.

ACKNOWLEDGMENTS

Supported by the National Science Foundation, Hydrological Sciences Program (Grant EAR-0409756) at UIC, the U.S. Department of Energy; Office of Nuclear Physics (Contract DE-AC02-06CH11357) at Argonne National Laboratory; and WIPP programs administered by the U.S. Department of Energy, Office of Environmental Management at Sandia National Laboratories. Sandia National Laboratories is a multi-program laboratory managed and operated

by Sandia Corporation, a wholly owned subsidiary of Lockheed Martin Corporation, for the US Department of Energy's National Nuclear Security Administration under contract DE-AC04-94AL85000. The authors are grateful for insightful comments provided by Axel Suckow and an anonymous reviewer.

REFERENCES CITED

Beauheim, R.L., Ruskauff, G.J., 1998. Analysis of Hydraulic Tests of the Culebra and Magenta Dolomites and Dewey Lake Redbeds Conducted at the Waste Isolation Pilot Plant Site. SAND98-0049; Sandia National Laboratories, Albuquerque, NM.

Bethke, C.M., Johnson, T.M., 2008. Groundwater age and groundwater age dating. Ann. Rev. Earth Planet. Sci. 36,121–52.

Chen, C.-Y., Li, Y.M., Bailey, K., O'Connor, T. P., Young, L., Lu Z.-T., 1999. Ultrasensitive isotope trace analysis with a magneto-optical trap. Science 286, 1139-1141.

Collon, P., Kutschera, W., Lu Z.-T., 2004. Tracing noble gas radionuclides in the environment. Ann. Rev. Nucl. Part. Sci. 54, 39-67.

Cook, P.G., Love, A.J., Robinson, N.I., Simmons, C .T., 2005. Groundwater ages in fractured rock aquifers. J. Hydrol. 308, 284–301.

Dubasov, Y.V., Okunev, N.S., 2010. Krypton and xenon radionuclides monitoring in the northwest region of Russia. Pure Appl. Geophys. 167, 487-498.

Grizak, G.E., Pickens, J.F., 1980. Solute transport through fractured media 1. The effect of matrix diffusion. Water Resourc. Res. 16, 719-730.

Haggerty, R.W., Fleming, S.W., Meigs, L.C., McKenna, S.A., 2001. Tracer tests in a fractured dolomite 2. Analysis of mass transfer in single-well injection-withdrawal tests. Water Resour. Res. 37, 1129-1142.

Hart, D.B., Holt, R.M., McKenna, S.A., 2008. Analysis Report for Task 5 of AP-114: Generation of Revised Base Transmissivity Fields. ERMS 549597; Sandia National Laboratories, Carlsbad, NM.

Holt, R.M., 1997. Conceptual model for transport processes in the Culebra Dolomite Member, Rustler Formation. SAND97-0194; Sandia National Laboratories, Albuquerque, NM.

Helton, J.C., Anderson, D.R., Jow, H.-N., Marietta, M.G., Basabilvazo, G., 1999. Performance Assessment in Support of the 1996 Compliance Certification Application for the Waste Isolation Pilot Plant. Risk Analysis 19(5), 959-986.

Jähne, B., Heinz, G., Dietrich, W., 1987. Measurement of the diffusion coefficients of sparingly soluble gases in water. J. Geophys. Res. 92, 10767-10776.

Jiang, W., Bailey, K., Lu, Z.-T., Mueller, P., O'Connor, T.P., Cheng, C.-F., Hu, S.-M., Purtschert, R., Sturchio, N.C., Sun, Y.R., Williams, W.D., Yang, G.-M, 2012. ATTA-3: An atom counter for measuring ^{81}Kr and ^{85}Kr in environmental samples. Geochim. Cosmochim. Acta 91, 1-6.

Kuhlman, K.L., Barnhart, K.S., 2011. Hydrogeology Associated with the Waste Isolation Pilot Plant; International High-Level Radioactive Waste Management Conference, Paper 3317; American Nuclear Society, Albuquerque, NM.

Lambert, S. J., 1987. Feasibility Study: Applicability of Geochronologic Methods Involving Radiocarbon and Other Nuclides to the Groundwater Hydrology of the Rustler Formation. SAND86-1054; Sandia National Laboratories, Albuquerque, NM.

Lambert, S.J., 1992. Geochemistry of the Waste Isolation Pilot Plant (WIPP) site, Southeastern New Mexico, USA. Appl. Geochem. 37(6), 513-531.

Lehmann, B.E., Love, A., Purtschert, R., Collon, P., Loosli, H.H, Kutschera, W., Beyerle, U., Aeschbach-Hertig, W., Kipfer, R., Frape, S.K., Herczeg, A., Moran, J., Tolstikhin, I.N., Gröning, M.A., 2003. Comparison of groundwater dating with ^{81}Kr, ^{36}Cl and ^{4}He in four wells of the Great Artesian Basin, Australia. Earth Planet. Sci. Lett. 211, 237-250.

Maloszewski, P., Zuber, A., 1991. Influence of matrix diffusion and exchange reactions on radiocarbon ages in fissured carbonate aquifers. Water Resour. Res. 27, 1937–1945.

McKenna, S.A., Meigs, L.A., Haggerty, R., 2001. Tracer tests in a fractured dolomite 3. Double-porosity, multiple-rate mass transfer processes in convergent flow tracer tests. Water Resour. Res. 37(5), 1143-1154.

Meigs, L., Beauheim, R., 2001. Tracer tests in a fractured dolomite,1. Experimental design and observed tracer recoveries. Water Resour. Res. 37, 1113-1128.

Momoshima, N., Inoue, F., Sugihara, S., Shimada, J., Taniguchi, M., 2010. An improved method for ^{85}Kr analysis by liquid scintillation counting and its application to atmospheric ^{85}Kr determination. J. Environ. Radioactivity 101, 615-621.

Mora, C.J., 1999. Sandia and the Waste Isolation Pilot Plant 1974-1999. SAND99-1482; Sandia National Laboratories, Albuquerque, NM.

Neretnieks, I., 1980. Diffusion in the rock matrix: An important factor in radionuclide retardation. J. Geophys. Res. 85, 4379-4397.

Neretnieks, I., 1981. Age dating of groundwater in fissured rock: Influence of water volume in micropores. Water Resour. Res. 17, 421-422.

Newman, B.D., Osenbrück, K., Aeschbach-Hertig, W., Solomon, D.K., Cook, P., Różański, K., Kipfer, R., 2010. Dating of "young" groundwaters using environmental tracers: Advantages, applications, and research needs. Isotopes Environ. Health Studies 46, 259-278.

Phillips, F.M., 2000. Chlorine-36. In Environmental Tracers in Subsurface Hydrology; Cook, P.G., Herczeg, A.L., Eds.; Kluwer Academic Press: Boston.

Plummer, L.N., Busenberg, E., 2008. Evaluation of Selected Environmental Tracer Data in Ground Water from Seven Wells in the Vicinity of the WIPP Site, New Mexico under Contract #586712 between the US Geological Survey and Sandia National Laboratories. ERMS 561539; Sandia National Laboratories, Carlsbad, NM.

Plummer, L.N., Glynn, P.D., 2013. Radiocarbon dating in groundwater systems. In Isotope Methods for Dating Old Groundwater (A. Suckow, P. Aggarwal, and L. Araguas-Araguas, Eds.), pp. 33-90. International Atomic Energy Agency, Vienna, Austria.

Plummer, L.N., Sprinkle, C.L., 2001. Radiocarbon dating of dissolved inorganic carbon in groundwater from confined parts of the Upper Floridan aquifer, Florida, USA. Hydrogeol. J. 9, 127-150.

Powers, D.W., 2009. Basic Data Report for Drillhole SNL-8 (C-3150) (Waste Isolation Pilot Plant). DOE/WIPP 05-3324; U. S. Department of Energy, Carlsbad, NM.

Powers, D.W., Holt, R.M., 2000. The salt that wasn't there: mudflat facies equivalents to halite of the Permian Rustler Formation, southeastern New Mexico. J. Sediment. Res. 70(1), 29-36.

Powers, D.W., Richardson, R.G., 2008. Basic Data Report for Drillhole SNL-14 (C-3140) (Waste Isolation Pilot Plant). DOE/WIPP 05-3320; U. S. Department of Energy, Carlsbad, NM.

Probst, P.C., Yokochi, R., Sturchio, N.C., 2007. Method for extraction of dissolved gases from groundwater for radiokrypton analysis. In Proceedings of the 4th Mini Conference on Noble Gases in the Hydrosphere and in Natural Gas Reservoirs; GFZ Helmholtz Center: Potsdam, Germany. Available at http://bib.gfz-potsdam.de/pub/minoga/minoga_conference_proceedings_070215-c.pdf; Accessed July 26, 2013).

Sanford, W., 1997. Correcting for diffusion in carbon-14 dating of groundwater. Ground Water 35, 357–361.

Siegel, M.D., Anderholm, S., 1994. Geochemical evolution of groundwater in the Culebra Dolomite near the Waste Isolation Pilot Plant, southeastern New Mexico, USA. Geochim. Cosmochim. Acta 58, 2299-2233.

Sturchio, N.C., Du, X., Purtschert, R., Lehmann, B.E., Sultan, M., Patterson, L.J., and 12 others, 2004. One million year old groundwater in the Sahara revealed by ^{81}Kr and ^{36}Cl. Geophys. Res. Lett. 31, L05503.

Suckow, A., Aggarwal, P., Araguas-Araguas, L., 2013. Isotope Methods for Dating Old Groundwater. STI/PUB/1587; International Atomic Energy Agency, Vienna, Austria, 356 p.

Suckow, A., Sonntag, C., 1993. The influence of salt on the noble gas thermometer. In: Isotope Techniques in the Study of Past and Current Environmental Changes in the Hydrosphere and the Atmosphere. International Atomic Energy Agency, Vienna, pp. 307- 318.

Sudicky, E.A., Frind, E.O., 1981. Carbon-14 dating of groundwater in confined aquifers: implications of aquitard diffusion. Water Resour. Res. 17, 1060–1064.

Swift, P.N., Corbet, T.F., 2000. The geologic and hydrogeologic setting of the Waste Isolation Pilot Plant. Reliability Eng. Syst. Safety 69, 47-58.

Tang, D.H., Frind, E.O., Sudicky, E.A., 1981. Contaminant transport in fractured porous media: Analytical solution for a single fracture. Water Resour. Res. 17, 555–564.

U.S. DOE, 2014. Appendix TFIELD in Title 40 CFR Part 191 Subparts B and C Compliance Recertification Application for the Waste Isolation Pilot Plant. DOE/WIPP 14-3503; US Department of Energy, Carlsbad Field Office, Carlsbad, NM..

Wise, D.L., Houghton, G., 1968. Diffusion coefficients of neon, krypton, xenon, carbon monoxide and nitric oxide in water at 10-60°C. Chem. Eng. Sci. 23, 1211-1216.

Yang G.-M., Cheng C.-F., Jiang W., Lu, Z.-T., Purtschert R., Sun Y.-R., Tu L.-Y., Hu S.-M., 2013. Analysis of ^{85}Kr: a comparison at the 10^{-14} level using micro-liter samples. Sci. Rep. 3, 1596.

Yokochi, R., Heraty, L.J., Sturchio, N.C., 2008. Method for purification of krypton from environmental samples for radiokrypton analysis. Anal. Chem. 80, 8688–8693.

FIGURE CAPTIONS

Figure 1. Location map showing WIPP repository site in southeastern New Mexico. The inset map with scale shows Nash Draw, Clayton Basin, and WIPP Culebra wells SNL-8 and SNL-14.

Figure 2. WIPP site stratigraphy schematically portrayed in a SW-NE cross-section through the site.

Figure 3. Particle tracks from the upstream model boundary (R) to SNL-14 (red tracks); each track corresponds to an individual model realization. The WIPP land-withdrawal boundary is a black square. Black dots are locations of monitoring wells used in calibration of the groundwater flow model. The background color flood and flow vectors indicate the speed and direction of flow averaged across all 100 realizations.

Figure 4. Histogram (solid line) of $\log_{10}$ travel times for 55 individual realizations (in 10,000-yr bins) from upstream flow model boundary (point R in Fig. 3) to well location SNL-14. Arrows indicate mode and mean of flow-model travel times, and ^{81}Kr model age (shown as dashed line, with dotted lines indicating errors based on counting statistics).

Figure 5. Solutions of equations (6) and (7) for a range of stagnant zone widths (w_{stag}) at fixed values of flow zone width (w_{flow} = 4.4 m), flow zone porosity (φ = 0.15), and aqueous Kr diffusivity (D_{aq} = 6.3 x 10^{-2} m^2 yr^{-1}). Values of t_u/t_c (uncorrected age/corrected age in years) assume the ^{81}Kr model age determined for SNL-14 (t_u = 132,000 yr). Results imply relatively

low values for D_{eff} (effective diffusivity of Kr) in the thick (> 30 m) stagnant zone around the Culebra Dolomite.

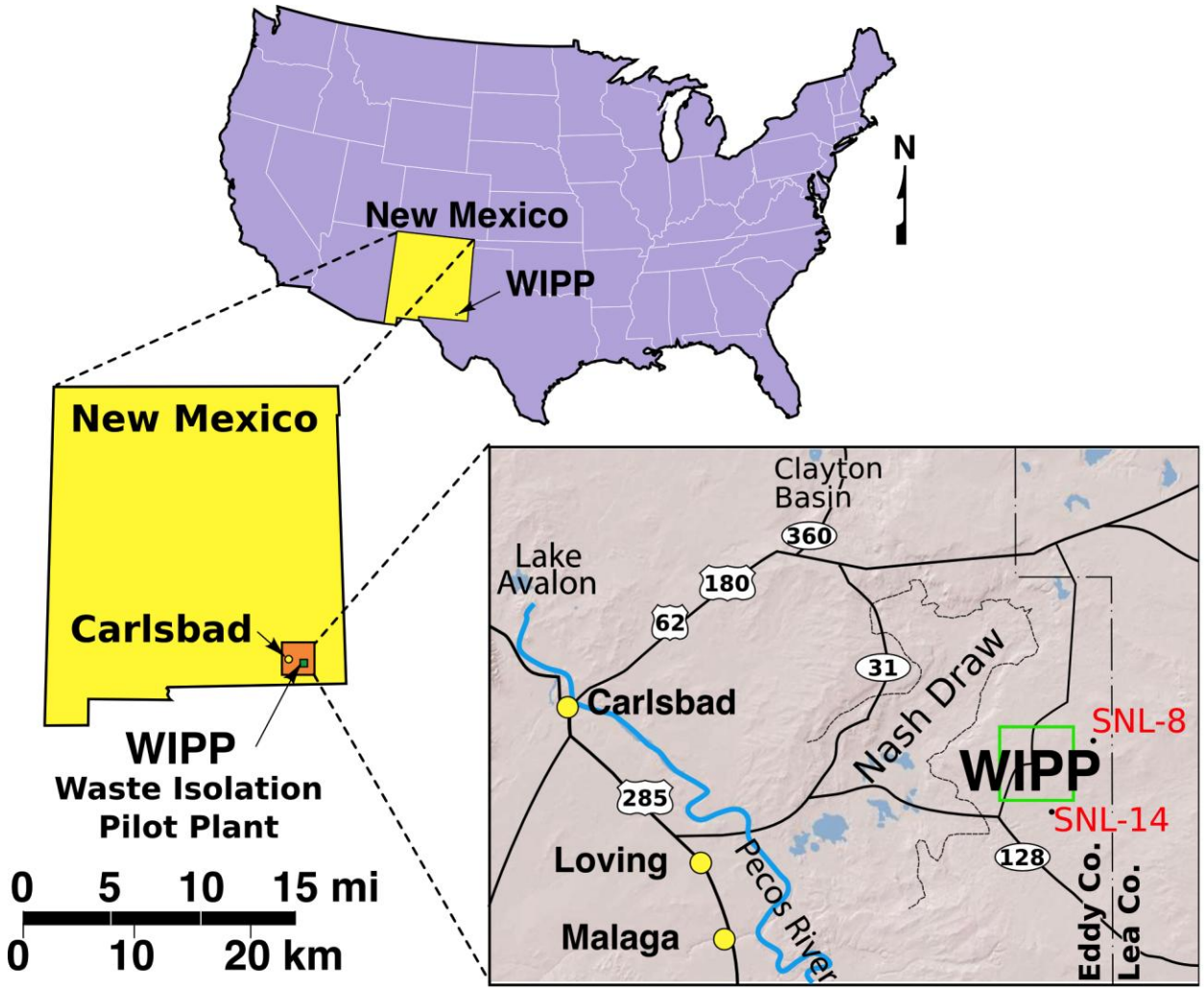
New Mexico
WIPP
N
New Mexico
Carlsbad
WIPP
Waste Isolation
Pilot Plant
0 5 10 15 mi
0 10 20 km
Clayton
Basin
Lake
Avalon
360
180
62
31
Carlsbad
Nash Draw
SNL-8
WIPP
SNL-14
285
128
Loving
Pecos River
Malaga
Eddy Co.
Lea Co.

Figure 1.

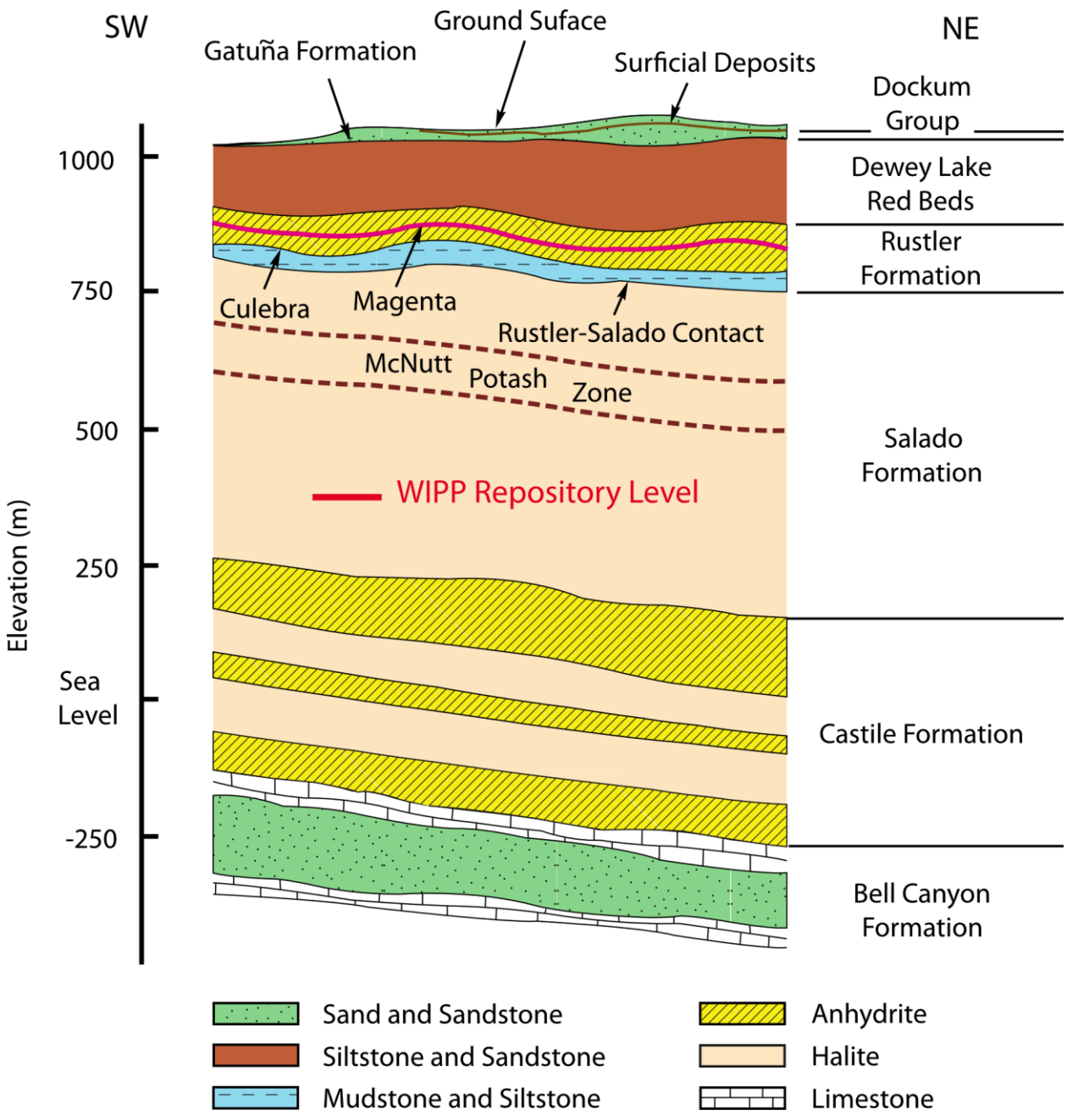
SW
NE
Ground Suface
Gatuña Formation
Surficial Deposits
Dockum Group
Dewey Lake Red Beds
Rustler Formation
Salado Formation
Castile Formation
Bell Canyon Formation
Elevation (m)
1000
750
500
250
Sea Level
-250
Culebra
Magenta
Rustler-Salado Contact
McNutt Potash Zone
WIPP Repository Level
Sand and Sandstone
Siltstone and Sandstone
Mudstone and Siltstone
Anhydrite
Halite
Limestone

Figure 2.

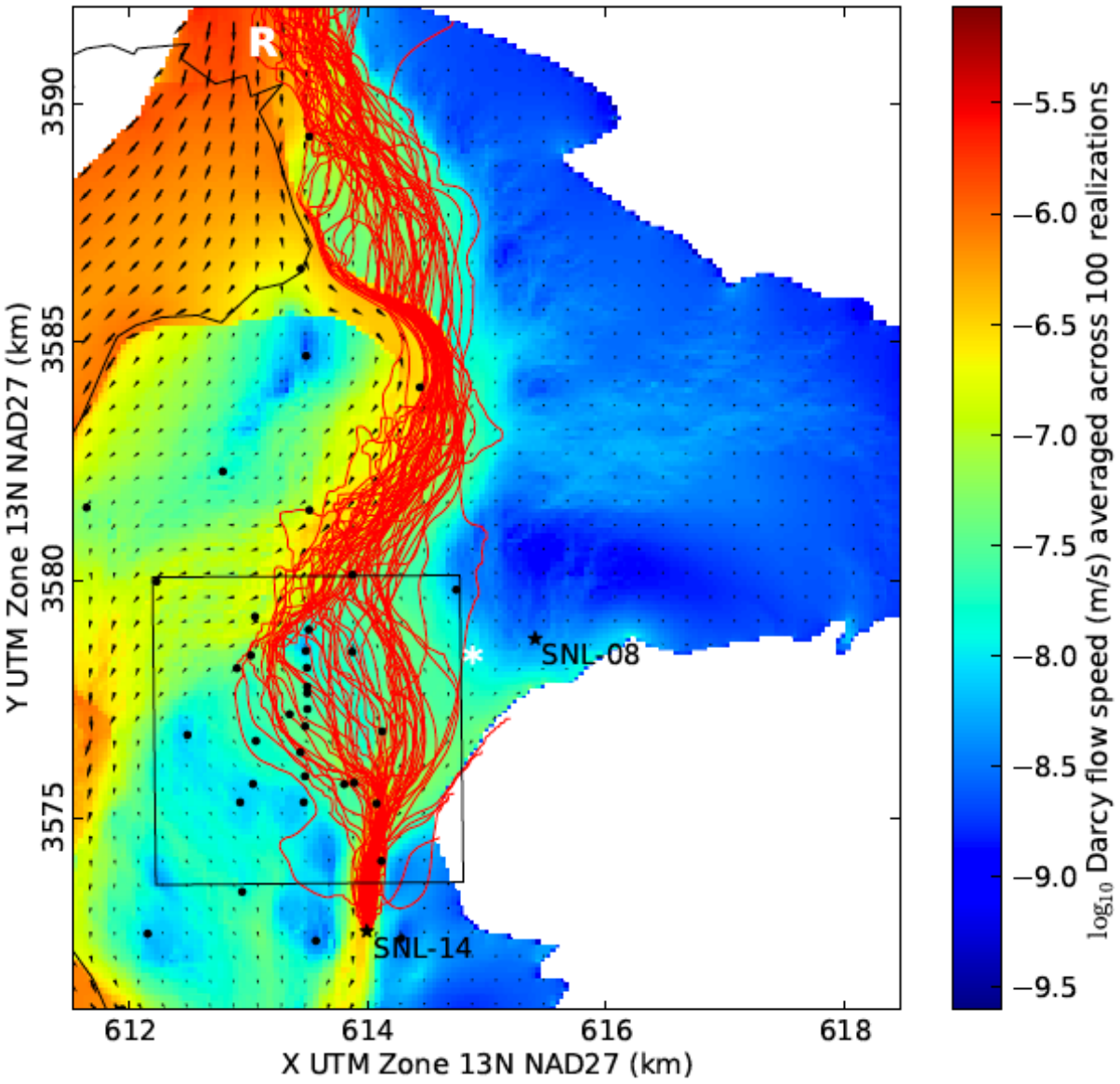
R
SNL-08
SNL-14
3590
3585
3580
3575
612
614
616
618
Y UTM Zone 13N NAD27 (km)
X UTM Zone 13N NAD27 (km)
−5.5
−6.0
−6.5
−7.0
−7.5
−8.0
−8.5
−9.0
−9.5
log10 Darcy flow speed (m/s) averaged across 100 realizations

Figure 3.

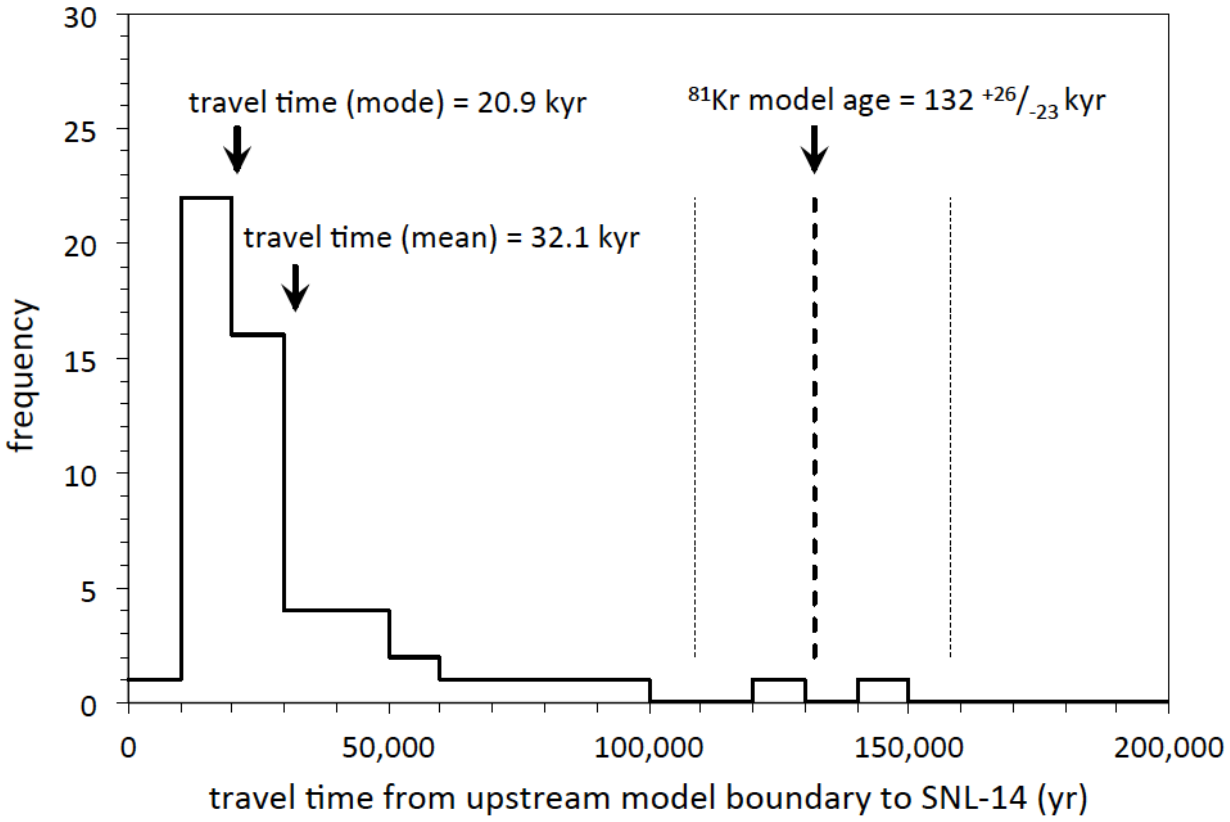
travel time (mode) = 20.9 kyr
81Kr model age = 132 +26/-23 kyr
travel time (mean) = 32.1 kyr
frequency
30
25
20
15
10
5
0
0
50,000
100,000
150,000
200,000
travel time from upstream model boundary to SNL-14 (yr)

Figure 4.

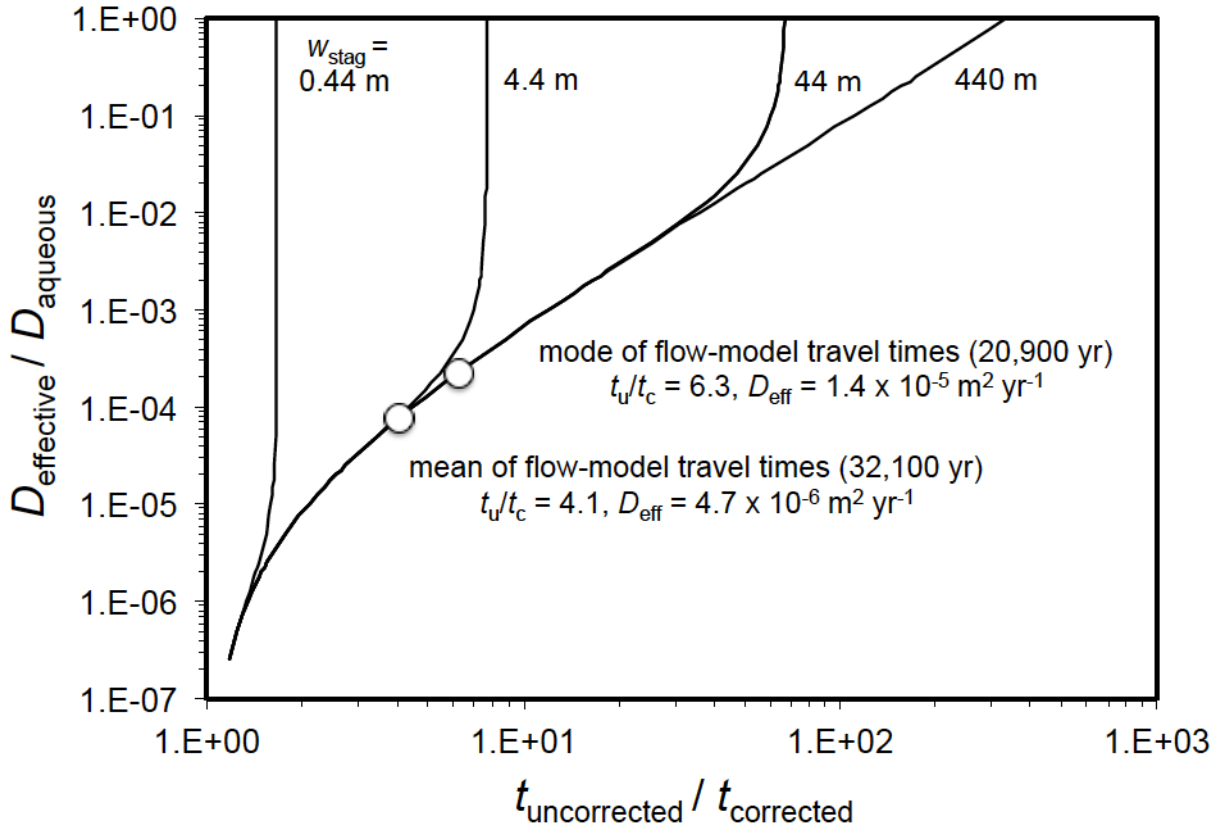
1.E+00
1.E-01
1.E-02
1.E-03
1.E-04
1.E-05
1.E-06
1.E-07
$D_{effective}$ / $D_{aqueous}$
w_{stag} = 0.44 m
4.4 m
44 m
440 m
mode of flow-model travel times (20,900 yr)
t_u/t_c = 6.3, D_{eff} = 1.4 x 10^{-5} m^2 yr^{-1}
mean of flow-model travel times (32,100 yr)
t_u/t_c = 4.1, D_{eff} = 4.7 x 10^{-6} m^2 yr^{-1}
1.E+00
1.E+01
1.E+02
1.E+03
$t_{uncorrected}$ / $t_{corrected}$

Figure 5.

Table 1. Sample and Analytical Data for Culebra Dolomite Groundwaters

	SNL-8	SNL-14
sampling parameters		
well completion date	7/6/05	6/1/05
pump depth, mbgs*	294	202
screened interval, mbgs	290-298	198-206
sampling dates	7/31-8/1/07	7/30/07
sample time, hours	28.3	5.0
water extracted, L	2997	5138
pumping rate, L min^{-1}	1.9	16.3
water-quality data		
T, ^{o}C	24	27
pH	7.41	7.26
Na, mg L^{-1}	30,000	47,000
K, mg L^{-1}	620	1,500
Mg, mg L^{-1}	1,100	3,100
Ca, mg L^{-1}	1,500	2,000
Sr, mg L^{-1}	22	33
Cl, mg L^{-1}	47,000	77,000
Br, mg L^{-1}	40	100
SO4, mg L^{-1}	6,900	6,400
alkalinity, mg L^{-1} (as $CaCO_3$)	48	49
TDS, mg L^{-1}	87,000	140,000
extracted gas composition		
N_2, volume %	96.79	98.23
O_2, volume %	0.08	0.04
Ar, volume %	1.19	1.35
CO_2, volume %	0.35	0.28
CH_4, volume %	0.16	0.04
radiokrypton data		
$(^{81}Kr/Kr_{sample})/(^{81}Kr/Kr_{atmosphere})$	0.50 ± 0.04	0.67 ± 0.05
$(^{81}Kr/Kr_{sample})/(^{81}Kr/Kr_{atmosphere})$**	0.37 ± 0.05	0.67 ± 0.05
^{85}Kr (decay min^{-1} cm^{-3})#	13.6 ± 1.1	<2.1
other isotopic tracer data##		
Tritium (TU)	0.10 ± 0.10	0.13 ± 0.13
^{14}C, DIC (pmc)	13.06 ± 0.15	6.94 ± 0.12

* mbgs -- meters below ground surface
** corrected for Kr introduced during well con
# corrected for time between sample collection and analysis
from Plummer and Busenberg (2008)